THE JOURNAL OF BIOLOGICAL CHEMISTRY VOL. 290, NO. 15, pp. 9738–9752, April 10, 2015

Sestrin 2 Protein Regulates Platelet-derived Growth Factor Receptor β (Pdgfrβ) Expression by Modulating Proteasomal and Nrf2 Transcription Factor Functions*

Received for publication, December 11, 2014, and in revised form, February 20, 2015 Published, JBC Papers in Press, February 25, 2015, DOI 10.1074/jbc.M114.632133

Ana Tomasovic[‡], Nina Kurrle[‡], Duran Sürün[‡], Juliana Heidler[‡], Koraljka Husnjak[§], Ina Poser[¶], Frank Schnütgen[‡], Susan Scheibe[‖], Michael Seimetz[‖], Peter Jaksch[**], Anthony Hyman[¶], Norbert Weissmann[‖], and Harald von Melchner[‡1]

*From the [‡]Department of Molecular Hematology, Goethe University Medical School, 60590 Frankfurt am Main, Germany, [§]Institute of Biochemistry II, Goethe University Medical School, 60590 Frankfurt am Main, Germany, [¶]Max Planck Institute of Molecular Cell Biology and Genetics, 01307 Dresden, Germany, [‖]Excellence Cluster Cardiopulmonary System (ECCPS), Justus-Liebig-University Giessen, Department of Internal Medicine, Universities of Giessen and Marburg Lung Centre (UGMLC), 35392 Giessen, Germany, and **Department of Thoracic Surgery, University Hospital of Vienna, A-1090 Vienna, Austria*

Background: Sestrin 2 is a redox-dependent repressor of Pdgfrβ signaling and thereby interferes with lung injury repair.
Results: Sestrin 2 is a positive regulator of proteasomal function and activates transcription of Nrf2-regulated antioxidant genes.
Conclusion: Sestrin 2 is a component of a novel Sestrin 2/Pdgfrβ repressor pathway.
Significance: The Sestrin2/Pdgfrβ repressor pathway is likely to play role in the pathogenesis of chronic obstructive pulmonary disease (COPD).

We recently identified the antioxidant protein Sestrin 2 (Sesn2) as a suppressor of platelet-derived growth factor receptor β (Pdgfrβ) signaling and Pdgfrβ signaling as an inducer of lung regeneration and injury repair. Here, we identified Sesn2 and the antioxidant gene inducer nuclear factor erythroid 2-related factor 2 (Nrf2) as positive regulators of proteasomal function. Inactivation of Sesn2 or Nrf2 induced reactive oxygen species-mediated proteasomal inhibition and Pdgfrβ accumulation. Using bacterial artificial chromosome (BAC) transgenic HeLa and mouse embryonic stem cells stably expressing enhanced green fluorescent protein-tagged Sesn2 at nearly endogenous levels, we also showed that Sesn2 physically interacts with 2-Cys peroxiredoxins and Nrf2 albeit under different reductive conditions. Overall, we characterized a novel, redox-sensitive Sesn2/Pdgfrβ suppressor pathway that negatively interferes with lung regeneration and is up-regulated in the emphysematous lungs of patients with chronic obstructive pulmonary disease (COPD).

Sestrin 2 belongs to a family of highly conserved, stress-inducible proteins implicated in the regulation of metabolic homeostasis. Mammalian cells express three sestrin isoforms: sestrin 1 (Sesn1[2]; also known as PA26), sestrin 2 (Sesn2; also known as Hi95), and sestrin 3 (Sesn3) (1, 2); Sesn1 and Sesn2 are involved in the defense against reactive oxygen species (ROS). The antioxidant function of the sestrins was originally attributed to their sulfinic acid reductase activity required for regenerating over-oxidized 2-Cys-peroxiredoxins (Prxs) (3). Prxs are highly conserved and ubiquitously expressed antioxidant proteins that are inactivated by hyperoxidation of their peroxidatic cysteine, thus yielding sulfinic acid in the presence of high peroxide concentrations (4, 5). However, it was later shown that the primary Prx reactivating enzyme is sulfiredoxin, which unlike the typical cellular reductants such as glutathione or thioredoxin can reduce sulfinic acid to thiol (6, 7). Therefore, the ability of Sesn1 and -2 to catalyze sulfinic to sulfenic acid is still a matter of debate.

Antioxidant activities of Sesn1 and -2 were recently attributed to their activation of the Nrf2 (nuclear factor erythroid 2-related factor 2)-Keap1 (Kelch-like ECH-associated protein 1) pathway (7). Nrf2 is a global antioxidant gene inducer whose activity is tightly controlled by cytoplasmic association with its inhibitor, Keap1. Keap1 targets Nrf2 for polyubiquitination and degradation by the 26 S proteasome, thereby keeping its basal levels low. Oxidative stress disrupts the Nrf2-Keap1 protein complex, and Nrf2 translocates into the nucleus where it heterodimerizes with its small Maf binding partner to transactivate antioxidant gene expression by binding the antioxidant response elements typically present in promoter regions of

* This work was supported by the SFB815 "Redox Signaling" of the Deutsche Forschungsgemeinschaft (DFG) and by individual grants from the DFG (ME 820-2) and the Else Kröner-Fresenius-Stiftung (2011-A47) (to H. v. M. and N. W.) and from the Bundesministerium für Bildung und Forschung (NGFN-plus-DiGtoP consortium/01GS0858 (to H. v. M. and A. H.). Additional support was received from the Excellence Cluster Cardiopulmonary System (ECCPS) and the Boehringer Ingelheim Foundation.

[1] To whom correspondence should be addressed. Tel.: 49-69-63016696; Fax: 49-69-63016390; E-mail: melchner@em.uni-frankfurt.de.

[2] The abbreviations used are: Sesn1 and Sesn2, sestrin 1 and 2, respectively; BAC, bacterial artificial chromosome; CHX, cycloheximide; CLA, chymotrypsin-like activity; COPD, chronic obstructive pulmonary disease; EGFP, enhanced GFP; ESC, embryonic stem cells; Gclc, glutamate-cysteine ligase catalytic subunit; nLAP, (N-terminal) localization and affinity purification tag; NAC, *N*-acetylcysteine; Nf-y, nuclear transcription factor complex Y; PDGF, platelet-derived growth factor; Pdgfrβ, platelet-derived growth factor receptor β; ROS, reactive oxygen species; SV40, simian virus 40; Prxs, peroxiredoxins; IF, immunofluorescence; IP, immunoprecipitate; MLF, mouse lung fibroblast; CMH, 1-hydroxy-3-methoxycarbonyl-2,2,5,5-tetramethylpyrrolidine; Sod, superoxide dismutase; Ho1, hemoxygenase 1; Nrf2, nuclear factor erythroid 2-related factor 2; Keap1, Kelch-like ECH-associated protein 1.

antioxidant genes (8). Sesn2 interfered with this pathway by stimulating the autophagic degradation of Keap1 (7).

Recently, we and others identified Sesn2 as a repressor of Pdgfrβ signaling (9, 10) and Pdgfrβ signaling as an inducer of lung tissue regeneration and injury repair (9). In mice, mutational inactivation of *Sesn2* prevents development of cigarette smoke-induced pulmonary emphysema by up-regulating Pdgfrβ-controlled alveolar maintenance programs (9). Although we showed that this up-regulation is mediated by ROS (9), the molecular mechanism(s) of this regulation was not determined.

The proteasome is the major site for removal of short-lived, unfolded, and damaged proteins. With a molecular weight of 150 MDa, the 26 S proteasome is one of the largest known catalytic complexes inside all eukaryotic cells. Composed of the catalytically active 20 S core and 19 S regulatory particles, the 26 S proteasome governs ubiquitin- and ATP-dependent protein degradation (11, 12). Three subunits of the 19 S proteasome (Rpt5, Rpn10, and Rpn13) bind polyubiquitinated substrates that earmark them for degradation (13–16). The catalytic centers are located inside the 20 S proteasome where three of its seven β-subunits show proteolytic activity, namely β1, β2, and β5, exhibiting caspase-, trypsin-, and chymotrypsin-like activities, respectively (17, 18). Oxidative stress leads to proteasome disassembly into its 19 S and 20 S subunits and to the accumulation of polyubiquitinated proteins (19).

Here we identify Sesn2 as a positive regulator of proteasomal function and the proteasome as a major component of a redox-sensitive signal transduction pathway controlling Pdgfrβ signaling. Within this pathway, we show that Nrf2 provides a crucial redox switch that, when activated by Sesn2, down-regulates Pdgfrβ by enhancing its proteasomal degradation. Finally, we show that this Sesn2/Pdgfrβ suppressor pathway is up-regulated in the emphysematous lungs of individuals with advanced chronic obstructive pulmonary disease (COPD), where it likely interferes with lung regeneration.

EXPERIMENTAL PROCEDURES

Reagents; Antibodies—Rabbit polyclonal antibodies against Sesn2 and Gclc were purchased from Proteintech Group (Manchester, UK). Rabbit polyclonal antibodies against Pdgfrβ (958; used for immunofluorescence (IF) and immunoprecipitation (IP)), PSMD1 (H-300), 20 S proteasome β1 (FL-241), 20 S proteasome β5 (H-47), c-myc, nuclear factor YA (NF-YA; G-2), Nrf2 (C-20; used for IF) and GFP as well as mouse monoclonal antibodies against ubiquitin (P4D1) and 20 S proteasome β2 (MCP 165) were from Santa Cruz Biotechnology (Heidelberg, Germany). Mouse monoclonal antibody against Nrf2 used for Western blot was obtained from R&D systems (clone #383727) (Minneapolis, MN). Mouse monoclonal antibodies against polyubiquitin chain (FK1) and 20 S α subunits (α1, -2, -3, -5, -6, and -7) were from Enzo Life Sciences (Lörrach, Germany). Rabbit monoclonal antibodies against DJ1, GAPDH, α-tubulin, hemoxygenase 1 (Ho1; P109), Keap1 (D6B12), MAP1LC3B (D11), and Pdgfrβ (28E1; used for Western blot) and mouse monoclonal antibody against p53 (1C12) were from Cell Signaling (Danvers, MA). Mouse monoclonal antibody against the His tag (C terminus) and β-actin were from Life Technologies and Sigma, respectively. Rabbit polyclonal antibodies against peroxiredoxin 1 (Prx1) and Prx-SO3 used for Western blots and IF were purchased from Abfrontier (Hamburg, Germany) and Abcam (Cambridge, UK), respectively. Mouse monoclonal antibodies against Prx2 were from Abfrontier (Hamburg, Germany). Cy3-conjugated goat anti-rabbit and Alexa Fluor 488 antibodies were from Dianova (Hamburg, Germany) and Molecular Probes (Darmstadt, Germany), respectively. Phalloidin-FITC was purchased from Molecular Probes and Cy3-streptavidin was from BioLegends (San Diego, CA). Secondary goat anti-mouse and goat anti-rabbit antibodies coupled to horseradish peroxidase (HRP) were from Santa Cruz Biotechnology and Sigma, respectively. Cytokines: hPDGF-BB (Sigma). Reagents Tempol (Tocris, Bristol, UK), H_2O_2, *N*-acetylcysteine (NAC), MG132, and chloroquine were all from Sigma.

Plasmids—Full-length Sesn2 was subcloned from human Sesn2-pLV-CMV plasmid (provided by Peter M. Chumakov, Lerner Research Institute, USA) into pGEX-4T1 (GE Healthcare, Uppsala, Sweden) for ectopic expression in BL21 bacterial strain. For ectopic expression of Sesn2 in mouse lung fibroblasts (MLFs), Sesn2 was cloned into the EcoRI site of pBabe-Puro (Cell Biolabs, Inc., San Diego, CA). Human β1 (PSMB6; NM_002798) was cloned into the BamHI site of pEGFP-N1. Ubiquitin-like (UBL) domain of hHR23B was cloned into the BamHI site of pGEX-4T1. The large T-antigen expression plasmid pSG5 was obtained from Addgene (#9053) (Cambridge, UK) (20). The doxycycline-inducible pRRL-ppT-SV40 large T antigen lentivirus used for the conditional immortalization of ES cell derived fibroblasts was a gift from Oezlem Demirel (Goethe University Frankfurt).

Cell Cultures and Cell Transductions—MLFs and HeLa, MRC5, and HEK293T cells were grown in Dulbecco's modified Eagle's medium (Life Technologies) supplemented with 10% (v/v) fetal calf serum (Life Technologies), 100 units/ml penicillin, and 100 μg/ml streptomycin (Life Technologies). HTBH-tagged hRpn11 expressing HEK293T cells (provided by L. Huang, University of California, Irvine) were used for affinity purification of human proteasomes. nLAP-Sesn2, Prx1, and Prx2 HeLa cell lines obtained from the BAC Interactomics resource (Hyman Lab, Max Planck Institute of Molecular Cell Biology and Genetics, Dresden, Germany) were grown in the presence of 400 μg/ml G418 (Life Technologies). nLAP-Sesn2 fibroblasts (nLAP-Sesn2 MF) were derived from murine nLAP-Sesn2 embryonic stem cells (21) by *in vitro* differentiation as described by Hewit *et al.* (22). Primary nLAP-Sesn2 MFs were conditionally immortalized by infecting the cells with the doxycycline-inducible pRRL-ppT-SV40 large T antigen lentiviral vector. Conditionally immortalized nLAP-Sesn2 MFs were maintained in standard tissue cultures supplemented with 1 μg/ml doxycycline (Sigma). Both wild type (WT) and *Nrf2* KO MLFs were isolated from the lungs of 4-month-old WT and *Nrf2* KO mice as described previously (23) and immortalized with SV40 large T antigen as described by Zalvide *et al.* (20). For transient transfections, HEK293T cells were plated on a 6-well plate, grown to 90% confluence, and transfected with 0.5 μg of β1-pEGFP-N1 plasmid using Lipofectamine 2000 according to the manufacturer's instructions (Life Technologies). Sesn2 KO MLFs stably re-expressing Sesn2 were obtained by infecting the cells with Sesn2-

pBabe-Puro retrovirus and selecting in 2 μg/ml puromycin (Life Technologies). shRNA knockdown of Sesn2 in MRC5 cells or Nrf2 in HeLa cells was performed by using the Mission Lentiviral *sh*RNA system (Sigma).

Cell Exposure to Growth Factors, Translational Inhibitors, Oxidants, and Antioxidants—For the activation of Pdgfrβ signaling, MLFs were serum-starved for 24 h before adding 25 ng/ml PDGF-BB to the cultures, as previously described (9). For Pdgfrβ half-life measurements, cells were exposed to 10 μg/ml cycloheximide (CHX with and without 5 mM Tempol or 10 μM MG132 or 100 μM chloroquine). Finally, for ROS level manipulations, cells were incubated with 125 μM H_2O_2 for 6 h unless otherwise stated or with 5 mM Tempol or NAC for 7 and 8 h, respectively.

Glutathione S-Transferase (GST) Protein Expression and Pulldown Assays—GST fusion proteins expressed in BL21 *Escherichia coli* strain were purified and coupled to glutathione-Sepharose beads (GE Healthcare) as previously described (25). For GST pulldown assays, MLFs and HEK293T cells were lysed on ice for 30 min in 50 mM Tris, pH 7.4, 0.15 M NaCl, 2 mM EDTA, 1% (v/v) Nonidet P-40 lysis buffer supplemented with Protease Inhibitor Mixture (Roche Applied Science). Cell lysates were incubated with either GST or GST-tagged proteins immobilized on glutathione-Sepharose beads overnight at 4 °C. The beads were washed 3 times with 1 ml of lysis buffer. The samples were resuspended in loading buffer containing 10% (v/v) β-mercaptoethanol, boiled for 5 min at 95 °C and separated by SDS-PAGE.

Immunofluorescence—Cells cultured on coverslips were fixed with 4% paraformaldehyde (Carl Roth), blocked, and permeabilized with 1% (w/v) BSA in PBS containing 0.5% (v/v) Triton X-100 (Carl Roth) or with 50 μg/ml digitonin (in DMSO; Carl Roth, Karlsruhe, Germany) for 15 min at room temperature. Cells were then sequentially labeled with primary and Cy3 and/or Alexa Fluor488-conjugated secondary antibodies. Stained cells were embedded in Fluoromount aqueous mounting medium (Sigma) supplemented with 1,4-diazadicyclo(2,2,2)-octane (50 mg/ml; Fluka, Taufkirchen, Germany). For visualizing the actin cytoskeleton and the nuclei, cells were counterstained with Phalloidin-FITC and DAPI, respectively. Samples were analyzed by using either a Zeiss LSM710 Confocal Laser scanning or a Leica TCS-SP5 microscope.

Co-immunoprecipitation—Cells were lysed for 30 min on ice in IP lysis buffer (10 mM Tris-HCl, pH 8, 150 mM NaCl, 5 mM EDTA, pH 8, 0.5% (v/v) Triton X-100, 60 mM *N*-octyglucopyranoside) supplemented with Roche Applied Science protease inhibitor mixture. For HTBH-hRpn11 IPs, lysates from HTBH-hRpn11 HEK293 cells were incubated with streptavidin agarose beads (Thermo Fisher Scientific, Waltham, MA) at 4 °C overnight, and unbound proteins were removed by washing once with IP lysis buffer supplemented with 1 mM ATP and 1 mM sodium orthovanadate and twice in Wash buffer (50 mM Tris-HCl, pH 7.5, 10% (v/v) glycerol) supplemented with 1 mM ATP and 1 mM sodium orthovanadate. For nLAP-Sesn2 IPs, cell lysates were incubated at 4 °C overnight with GFP Trap-A beads (Chromotek, Martinsried, Germany) and subsequently washed in IP lysis buffer. IPs were analyzed by SDS-PAGE and Western blotting.

Proteasome and Nrf2 Activity Assays—For measuring proteasome activity, cells were lysed on ice in proteasome activity lysis buffer (100 mM NaCl, 50 mM Na_3PO_4, 10% (v/v) glycerol, 5 mM $MgCl_2$, 0.5% (v/v) Nonidet P-40) supplemented with Protease Inhibitor Mixture (Roche Applied Science), 1 mM sodium orthovanadate, and 5 mM ATP (Sigma). The lysates were homogenized on ice by using a 23-gauge needle and cleared by centrifugation at 13,000 rpm for 15 min. Chymotrypsin-like activity was measured in duplicate using 50 μg of proteins and 100 μM succinyl-LLVY-amidomethylcoumarin (Enzo Life Sciences) fluorogenic substrate per reaction as previously described (14). Assays were carried out at 37 °C for 30 min, and activities were measured using a Viktor2 (PerkinElmer Life Sciences) spectrofluorometer with 380-nm excitation and 460-nm emission filters. For measuring proteasome activity in human lung samples, proteasome was purified from the tissue lysate by using the GST-tagged ubiquitin-like (UBL) domain of hHR23B. GST pulldown assays were performed overnight at 4 °C before proteasome activity measurements.

Nrf2 transactivation activity was estimated by using the Cignal Lenti antioxidant response element reporter (luc) assay (CLS-2020L) (Qiagen, Leipzig, Germany) according to the manufacturer's instructions. Briefly, MLFs were transiently transfected with the pCignal Lenti-TRE-Reporter plasmid. After 48 h, luminescence was measured by using a Mithras LB 940 plate reader (Berthold Technologies, Bad Wilbad, Germany).

ROS Measurements—Superoxide release from MLFs was measured by EPR as described (26). Briefly, EPR measurements were performed at −170 °C using an EMXmicro Electron Spin Resonance (ESR) spectrometer (Bruker, Karlsruhe, Germany) and 1-hydroxy-3-methoxycarbonyl-2,2,5,5-tetramethylpyrrolidine (CMH) (Noxygen, Elzach, Germany) as the spin probe for detecting intra- and extracellular superoxide production. Because CMH reacts with superoxide and peroxynitrite, parallel samples containing either CMH alone or CMH and superoxide dismutase (SOD) conjugated to polyethylene glycol (PEG-SOD) were measured. This enabled the assessment of the superoxide signal as part of the total CMH signal. Thus, duplicate samples of 2×10^5 cells were incubated with 15 units/ml PEG-SOD (Sigma) for 2 h at 37 °C followed by the addition of CMH (500 μM) ± PEG-SOD. After incubating for another 20 min, the samples were shock-frozen and stored in liquid nitrogen. Spectrometry was performed on frozen samples using a g-factor of 2.0063, a center field of 3349.95G, a microwave power of 200 milliwatt, a sweep time of 20 s, and a sweep number of 5.

Nucleic Acids and Protein Analyses—Total RNA was isolated by using the TriReagent kit (Sigma) according to the manufacturer's instructions. Lysates were centrifuged at 25,000 × *g* for 10 min at 4 °C. One microgram of RNA was reverse-transcribed in 20 μl of reverse transcription buffer containing 2 μM random primers (New England Biolabs, Frankfurt am Main, Germany) and 200 units of RevertAid H Minus Reverse Transcriptase (Thermo Fisher Scientific). Real time PCRs (Opticon 2 quantitative PCR machine, MJ Research, Ramsey, MN) were performed in duplicate in 25 μl of quantitative PCR SYBR Green Mix (Thermo Fisher Scientific) containing 5 μl of 5-fold diluted reverse transcription product using an annealing temperature of 60 °C. RNA polymerase II was used for normalization. Primer sequences are available on request.

Cell lysates and Western blotting for protein quantification were performed as previously described (9, 27). For protein

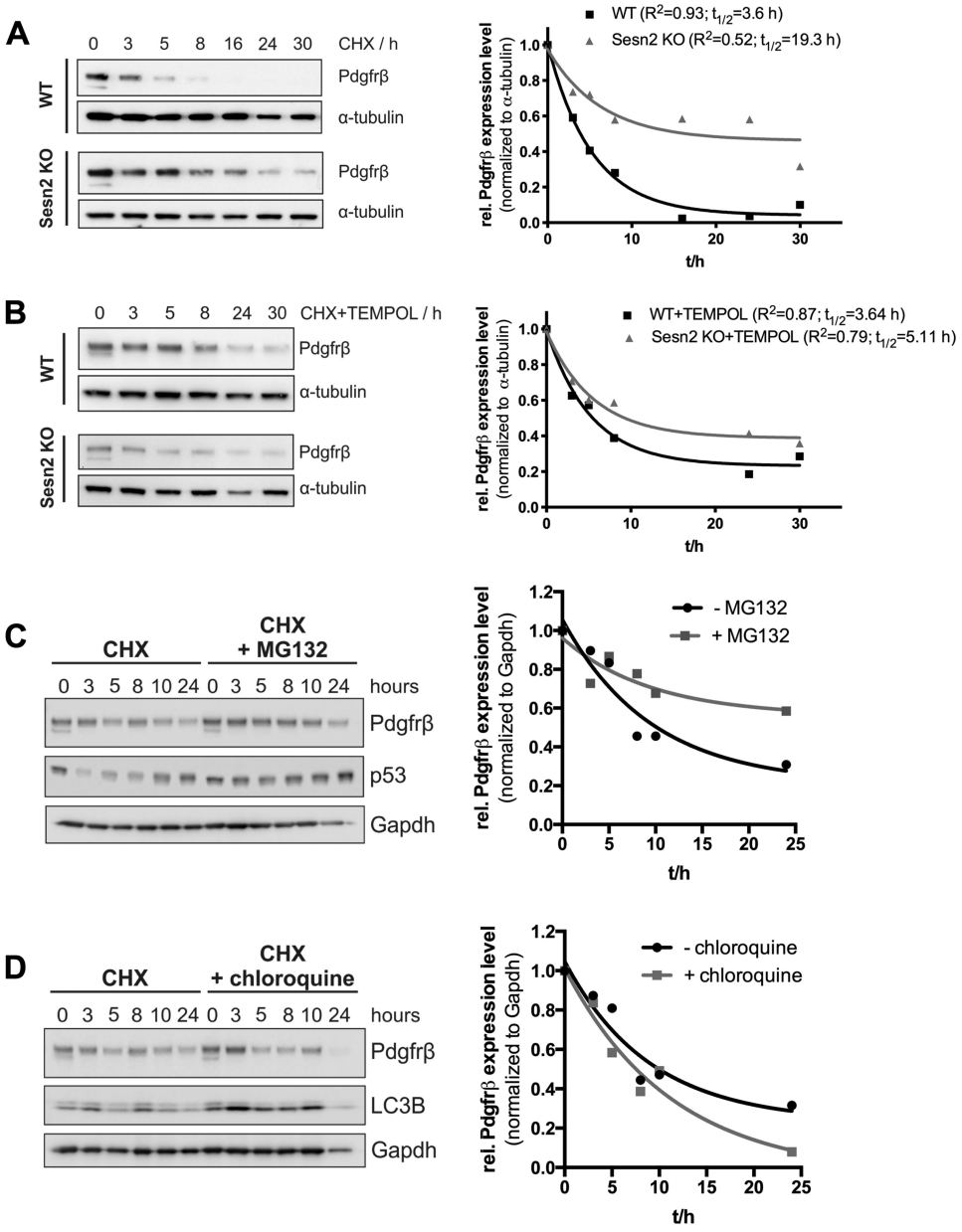

FIGURE 1. **Pdgfrβ half-life in *Sesn2* KO MLF.** *A*, Pdgfrβ levels in WT and *Sesn2* KO MLF exposed to CHX (10 μg/ml) for the indicated time intervals. *Left panel*, representative Western blot. *Right panel*, nonlinear regression analysis (one-phase exponential decay) of relative Pdgfrβ levels quantified by densitometry. *B*, Pdgfrβ levels in WT and *Sesn2* KO MLF exposed to CHX and Tempol. *Left panel*, representative Western blot. *Right panel*, nonlinear regression analysis of relative Pdgfrβ levels quantified by densitometry. *C*, Pdgfrβ levels in WT and *Sesn2* KO MLF exposed CHX $\pm$ MG132. *Left panel*, Western blot where p53 served as a positive control for proteasomal inhibition. *Right panel*, nonlinear regression analysis of relative Pdgfrβ levels quantified by densitometry. *D*, Pdgfrβ levels in WT and *Sesn2* KO MLF exposed to CHX $\pm$ chloroquine. *Left panel*, Western blot where LCB served as a positive control for lysosomal inhibition. *Right panel*, nonlinear regression analysis of relative Pdgfrβ levels quantified by densitometry.

analysis in PDGF-BB stimulation experiments, lysis buffers were supplemented with 1 mM each of sodium fluoride and sodium orthovanadate.

Patient Characteristics—Human lung tissues were obtained from COPD transplant patients (GOLD stage IV) and healthy donor controls (Table 1). The studies were approved by the Ethics Committee of the Justus-Liebig-University School of Medicine (AZ 31/93), Giessen, Germany.

Statistics—Comparisons between more than two groups were performed using analysis of variance (ANOVA) with the Bonferroni post-hoc test. For comparisons of two groups, Student's two-tailed *t* test was used. *p* values below 0.05 were considered significant.

RESULTS

Sesn2-depleted Mouse Lung Fibroblasts Accumulate Proteasomal Target Proteins—We and others showed that ROS and Pdgfrβ accumulate in MLFs from *Sesn2* knock out mice (*Sesn2* KO MLFs) (3, 9, 24). To test whether Pdgfrβ accumulation results from its decreased turnover, we estimated Pdgfrβ levels in MLFs at various time intervals after exposing the MLFs to the protein synthesis inhibitor CHX. Fig. 1*A* shows that Pdgfrβ

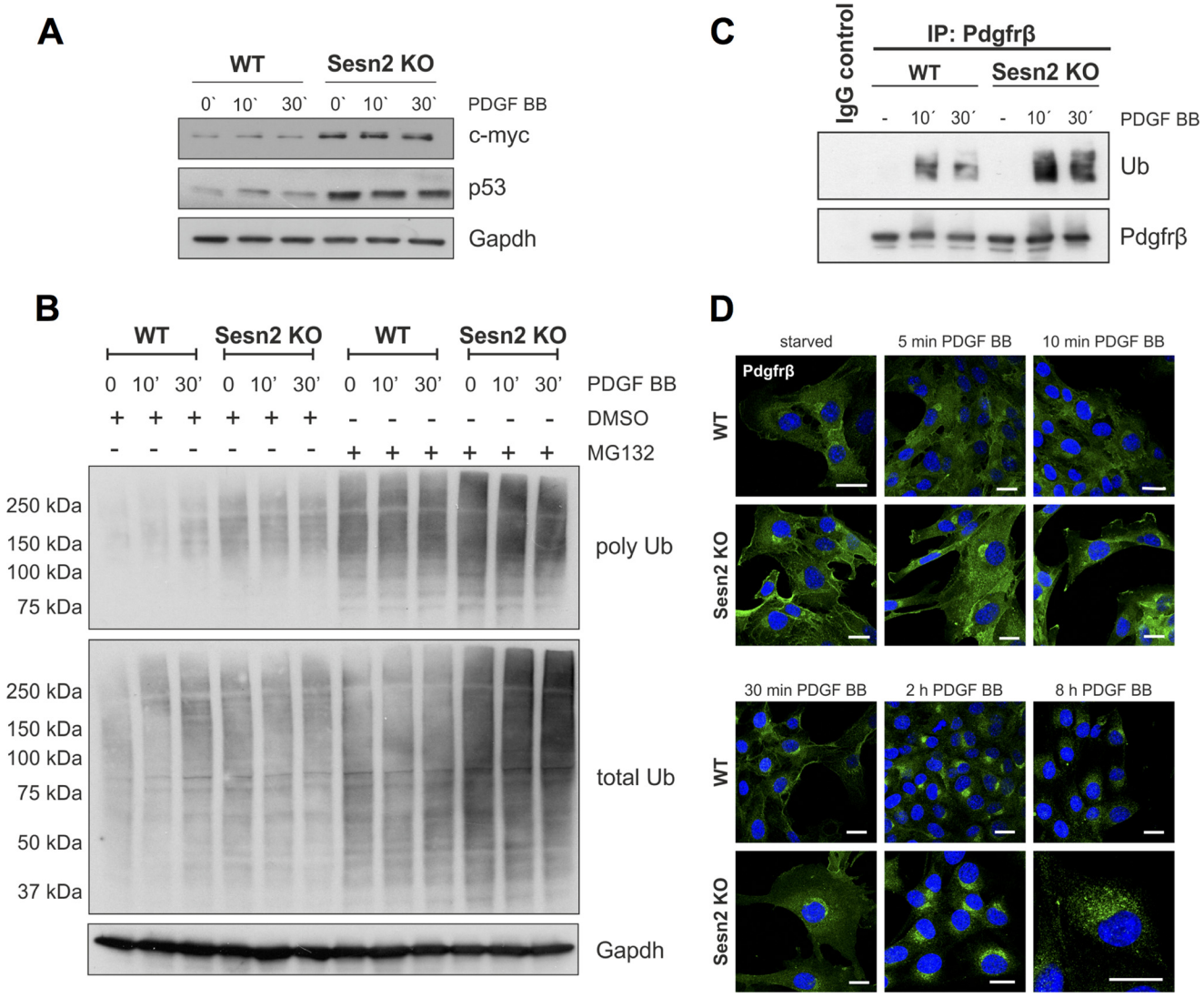

FIGURE 2. **Accumulation of proteasomal targets and polyubiquitinated proteins in *Sesn2* KO MLFs.** *A*, expression of c-myc and p53 in WT and *Sesn2* KO MLFs after stimulation with PDGF-BB for the indicated time intervals. *B*, polyubiquitinated protein levels in WT and *Sesn2* KO MLFs stimulated with PDGF-BB for the indicated time intervals in the presence or absence of the proteasomal inhibitor MG132. *C*, Pdgfrβ IPs from WT and *Sesn2* KO MLF probed with anti-Pdgfrβ and ubiquitin antibodies on Western blots. *D*, subcellular localization of Pdgfrβ (*green*) in WT and *Sesn2* KO MLFs after PDGF-BB stimulation. *Scale bar*: 20 μm.

levels declined about five times slower in *Sesn2* KO MLFs than in WT MLFs. However, the extended Pdgfrβ half-life in *Sesn2* KO MLFs could be readily reversed to normal by the ROS scavenger Tempol (Fig. 1*B*), indicating that the Pdgfrβ half-life prolongation is ROS-dependent.

Earlier studies showed that Pdgfrβ can undergo both lysosomal and proteasomal degradation (28, 29). To distinguish between these possibilities in our system, we treated MLFs exposed to CHX with chloroquine or MG132 to selectively inhibit lysosomal and proteasomal degradation, respectively. Fig. 1, *C* and *D*, show that MG132, but not chloroquine, prolonged the Pdgfrβ half-life in WT MLFs, indicating that Pdgfrβ degradation is primarily proteasomal.

Because excessive ROS negatively interfere with proteasomal function (19), we assumed that *Sesn2* KO MLFs exhibit defects in the proteasomal protein degradation system. To test this, we first estimated c-myc and p53 protein levels in WT and *Sesn2* KO MLFs by Western blotting. Because c-myc and p53 are exclusively degraded by the proteasome (30, 31), their steady state levels indirectly reflect proteasome activity. As shown in Fig. 2*A*, both c-myc and p53 accumulated in *Sesn2* KO MLFs, suggesting reduced proteasomal activity. This effect was independent of Pdgfrβ signaling, as c-myc and p53 levels remained unaffected by PDGF-BB ligand stimulation (Fig. 2*A*). Consistent with the reduced proteasomal activity, *Sesn2* KO MLFs accumulated polyubiquitinated proteins including Pdgfrβ (Fig. 2, *B* and *C*).

Next, we tested whether decreased receptor endocytosis might contribute to the elevated Pdgfrβ levels in *Sesn2* KO MLFs by monitoring subcellular Pdgfrβ localization at various time intervals after PDGF-BB stimulation. As shown in Fig. 2*D*, the kinetics of Pdgfrβ internalization after ligand stimulation were similar in WT and *Sesn2* KO MLFs, suggesting that its endocytosis is not affected by the *Sesn2* mutation. Taken together, the results suggest that Pdgfrβ accumulates in *Sesn2* KO MLFs as a result of a ROS-induced proteasome dysfunction.

Sesn2 Binds the Proteasome and Modulates Its Function—To confirm that proteasomal activity is reduced in the Sesn2-de-

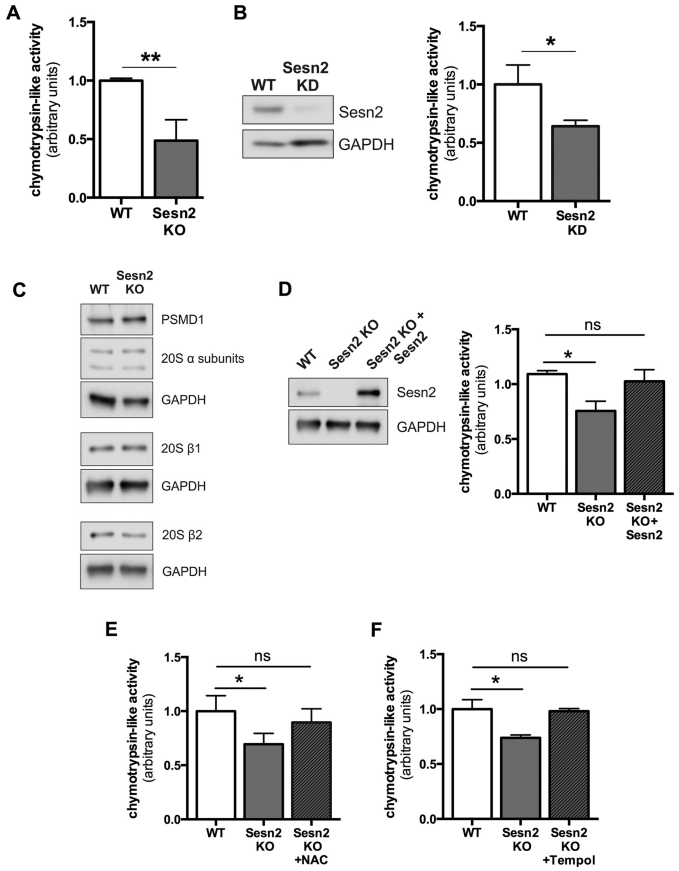

FIGURE 3. **Sesn2 modulates proteasomal function.** *A*, quantification of CLA in WT and *Sesn2* KO MLFs. CLA in *Sesn2* KO MLFs was normalized to the CLA of WT MLFs (=1). Results are represented as the means ± S.D. of three independent experiments. *B*, CLA in human embryonic lung fibroblasts (MRC5) transduced with anti-Sesn2 *shRNA*. *Left panel*, Western blot showing shRNA-mediated Sesn2 knock down efficiency in MRC5 cells. *Right panel*, CLA quantification in MRC5 cells. Results are represented as means ± S.D. of three independent experiments. *C*, Western blot showing the expression of proteasomal subunits in WT and *Sesn2* KO MLFs. *D*, CLA rescue in *Sesn2* KO MLFs overexpressing exogenous Sesn2. Sesn2 expression (*left panel*) and CLA (*right panel*) in WT, *Sesn2* KO, and Sesn2 reconstituted *Sesn2* KO MLFs (*KO* + *Sesn2*). *E* and *F*, CLA rescue in *Sesn2* KO MLFs by treatment with the antioxidants NAC (*E*) and Tempol (*F*) for 7 and 8 h, respectively. Results are represented as the means ± S.D. of three independent experiments. *, $p < 0.05$; **, $p < 0.01$. *ns*, not significant.

pleted cells, we measured chymotrypsin-like activity (CLA) in WT and *Sesn2* KO MLFs using the fluorogenic chymotrypsin substrate succinyl-LLVY-amidomethylcoumarin. As shown in Fig. 3*A*, *Sesn2* KO MLFs exhibited significantly decreased CLA when compared with WT MLFs. This was similar in human fetal lung fibroblasts (MRC5 cells) in which SESN2 was inactivated by *sh*RNA (Fig. 3*B*), suggesting that proteasomal inhibition is not restricted to murine cells.

Because expression levels of the α, β1, and β2 subunits of the 20 S proteasome as well as the levels of PSMD1 subunit of the 19 S proteasome were similar in *Sesn2* KO and WT MLFs (Fig. 3*C*), we concluded that the activity of the proteasome rather than the expression of the proteasomal subunits is affected by the *Sesn2* mutation. This activity could be restored in *Sesn2* KO MLFs by re-expressing Sesn2 (Fig. 3*D*) or by exposing the MLFs to the ROS scavengers NAC or Tempol (Fig. 3, *E* and *F*), suggesting that ROS contribute to proteasomal inhibition.

To test whether Sesn2 binds to the proteasome, we used HEK293T cells stably expressing a His-tagged, biotinylatable Rpn11 (HTBH-hRpn11) subunit of the 19 S proteasome (32) and pulled down Rpn11 by using streptavidin-coupled agarose beads. Western blot analysis identified Sesn2 in the pulldown in addition to the 19 S PSMD1 and 20 S α and β1 subunits, indicating that Sesn2 physically associates with the native proteasome (Fig. 4*A*). This association was supported further by IF stainings, which are suggestive of partial cytoplasmic and nuclear Sesn2/proteasome co-localization (Fig. 4*B*).

To investigate which proteasomal subunits bind to Sesn2, we performed GST pulldown assays from WT MLFs using a purified Sesn2-GST fusion protein bound to glutathione-Sepharose beads. As shown in Fig. 4*C*, Sesn2 bound to the α and catalytically active β1 and β5 subunits but not to the β2 and PSMD1 subunits of the 20- and 19 S proteasome, respectively. However, when testing β1 subunit binding, we observed a β1 band shift in the Sesn2-GST pulldown when compared with input (Fig. 4*C*). To verify that β1 indeed interacted with Sesn2, we performed additional GST pulldown assays from HEK293T cells transiently transfected with a GFP-tagged human β1 subunit expression plasmid. Fig. 4*D* shows that Sesn2-GST readily pulled down β1-GFP, but not GFP, confirming that Sesn2 physically interacts with the β1 subunit of the 20 S proteasome. Overall, these results suggest that Sesn2 may directly interfere with the proteolytic functions of the proteasome.

Sesn2 Interacts with 2-Cys Peroxiredoxins in a Redox-dependent Manner—It was suggested that Sesn2 reduces oxidative stress by binding to and reducing over-oxidized 2-Cys peroxiredoxins, in particular Prx1 and Prx2 (3). Because the Sesn2/Prx interactions were thus far detected only in exogenous protein overexpression experiments (3), we asked whether the interactions could also be detected under physiological conditions. For this, we used a HeLa cell line from the Bacterial Artificial Chromosome (BAC) Interactomics Resource stably expressing a BAC transgene in which the N terminus of SESN2 was tagged with an enhanced green fluorescent protein (EGFP) containing a localization and affinity purification (LAP) tag (nLAP-SESN2) (33). As nLAP-SESN2 is expressed and regulated like endogenous SESN2, these cells were amenable to generic tag-based proteomics under nearly physiological conditions.

We immunoprecipitated nLAP-SESN2 from the nLAP-Sesn2 HeLa cells using GFP-TrapA beads and probed the IPs with anti-Prx1, Prx2, and over-oxidized Prx (Prx-SO3) antibodies. Fig. 5*A* shows that PRX1 and PRX-SO3, but not PRX2, co-immunoprecipitated with nLAP-SESN2. Consistent with this finding, IF stainings of nLAP-Prx1 and nLAP-Prx2 HeLa cells obtained from the same BAC Interactomics resource showed cytosolic SESN2-PRX1 but not SESN2-PRX2 co-localization (Fig. 5*B*). Similarly, in nLAP-Sesn2 HeLa cells, SESN2 co-localized with endogenous PRX1 and PRX1-SO3 (Fig. 5*C*). However, this Sesn2/Prx interaction was inhibited by hydrogen peroxide (H_2O_2) (Fig. 5, *A* and *C*), which also induced translocation of SESN2 from the cytoplasm into the nucleus (Fig. 5*C*), implying that Sesn2 is not a Prx reductase.

We repeated these experiments using conditionally immortalized murine fibroblasts derived from an embryonic stem cell line expressing nLAP-Sesn2 from its endogenous locus (nLAP-

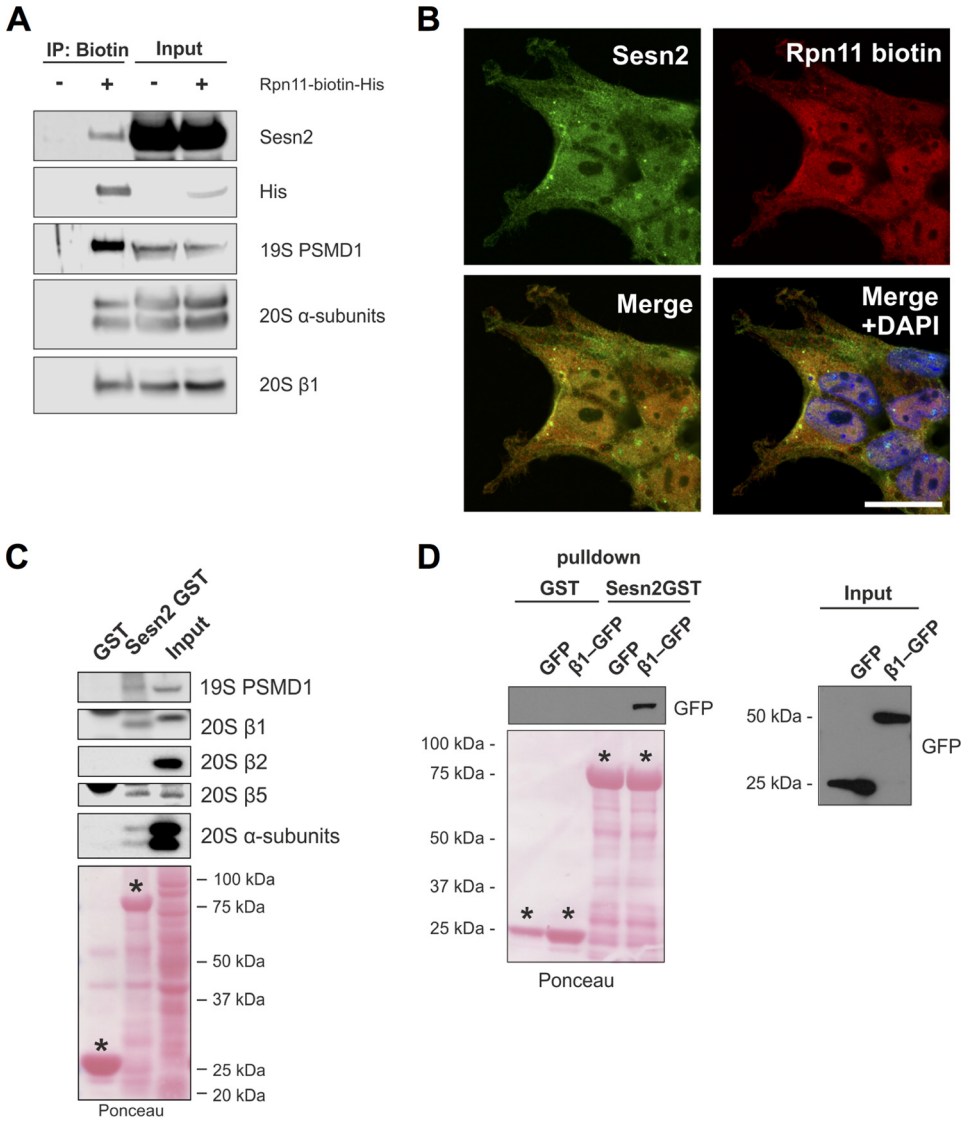

FIGURE 4. **Sesn2 associates with the proteasome.** *A*, native proteasome streptavidin pulldown assays from HTBH-hRpn11 HEK293 cells. Western blots were probed with antibodies against His, Sesn2, PSMD1, and 20 S β1 and α subunits. *B*, Rpn11 colocalization with endogenous Sesn2 in HTBH-hRpn11 HEK293 cells visualized by indirect immunofluorescence. *Scale bar*: 20 μm. *C*, Sesn2-GST pulldown assays from MLF lysates probed with antibodies against proteasomal subunits (*top panel*). The purified, GST, and full-length Sesn2-GST fusion proteins used for the pulldown assays are marked by *asterisks* on the *bottom panel*. *D*, Sesn2-GST pulldown assays from HEK293T cells expressing exogenous β1-GFP probed with GFP antibodies.

Sesn2-ESC) (21). Unlike the HeLa cells from the BAC Interactomics resource, the nLAP-Sesn2-ESCs were obtained by inserting the nLAP tag into a multipurpose Sesn2 gene trap allele by recombinase-mediated cassette exchange (21). Similar to the HeLa cells, the nLAP-Sesn2 of the conditionally immortalized fibroblasts (nLAP-Sesn2-MF) interacted with Prx1 and Prx-S03 in a redox-dependent manner (Fig. 5*D*). However, although nLAP-Sesn2-MFs did not express higher levels of Prx2 than the corresponding HeLa cells (Fig. 5*E*), Sesn2 interacted with Prx2 (Fig. 5*D*), suggesting that the basal Sesn2/Prx2 interaction is likely cell type-specific.

Nrf2 Activity Is Reduced by Sesn2 Inactivation—A recent study showed that Sesn2 activates the antioxidant transcription factor Nrf2 by binding and inactivating its inhibitor Keap1 (7). To test whether Nrf2 activity is compromised in Sesn2-depleted cells, we first estimated Nrf2 and Keap1 expression in WT and *Sesn2* KO MLFs by quantitative real-time-PCR and Western blotting. As shown in Fig. 6*A*, neither *Nrf2* nor Keap1 expression was affected by the loss of Sesn2. However, when the MLFs were subjected to antioxidant response elements (ARE)-luciferase reporter assay, *Sesn2* KO MLFs developed significantly less luciferase activity than the WT MLFs under both basal and oxidative stress conditions (Fig. 6*B*) and showed reduced expression of hemoxigenase 1 (Ho1), an endogenous Nrf2 target gene (Fig. 6*C*). These results suggest that ROS accumulate in Sesn2-deficient MLFs as a result of reduced Nrf2 activity and, consequently, inhibit proteasomal function.

Sesn2 Directly Interacts with Nrf2 in a Redox-dependent Manner—As noted above, Sesn2 activates Nrf2 by directly interacting with its inhibitor Keap1. However, this interaction was described in HEK293T cells overexpressing *Sesn2* and *Keap1* cDNAs (7). To test whether the Sesn2/Keap1 interaction can be replicated in cells expressing nearly normal levels of Sesn2, we immunoprecipitated nLAP-SESN2 from HeLa cells

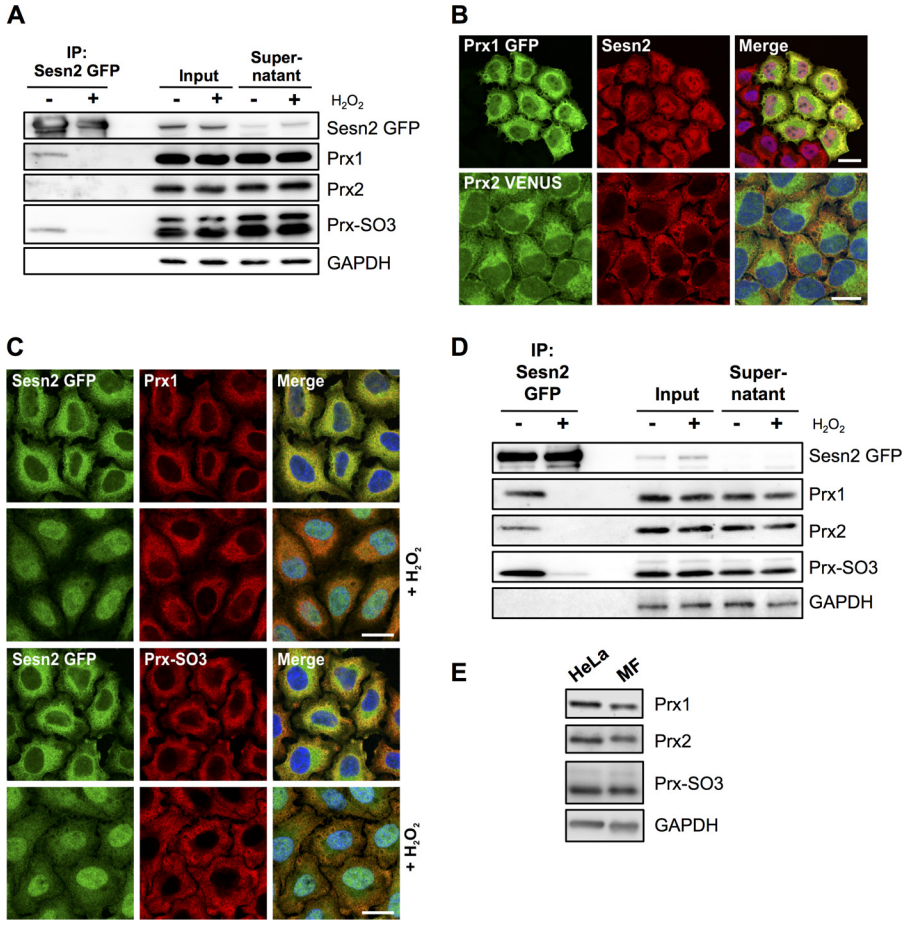

FIGURE 5. **Sesn2 binds Prxs in a redox-dependent manner.** *A*, nLAP-SESN2 IPs from HeLa cells probed with antibodies against GFP, Prx1, Prx2, and Prx-SO3 on Western blots. Where indicated, cells were exposed for 6 h to 125 μM H_2O_2 before immunoprecipitation. *B*, subcellular localization of Sesn2 and Prxs in nLAP-Prx1 and Prx2 HeLa cells visualized by EGFP autofluorescence and indirect immunofluorescence staining. Note Sesn2/Prx1 but not Sesn2/Prx2 colocalization in the cytosol. *Scale bar*: 20 μm. *C*, subcellular localization of Sesn2 and Prxs in nLAP-Sesn2 HeLa cells before and after treatment with H_2O_2. *Scale bar*: 20 μm. *D*, nLAP-Sesn2 IPs from nLAP-Sesn2 mouse fibroblasts probed with antibodies against Sesn2, Prx1, Prx2, and PrxSO3 on Western blots. Where indicated, cells were exposed for 6 h to 125 μM H_2O_2 before immunoprecipitation. *E*, expression of Prx1, Prx2, and Prx-SO3 in nLAP-Sesn2 HeLa (HeLa) and nLAP-Sesn2 MF (*MF*) cells.

either treated or untreated with H_2O_2 and probed the IPs with anti-Keap1 and Nrf2 antibodies. Fig. 6*D* shows that NRF2, but not KEAP1, co-immunoprecipitated with nLAP-SESN2, especially under oxidative stress conditions. Likewise, as revealed by IF staining, H_2O_2-induced SESN2-NRF2 co-localization and cytoplasmic nuclear translocation (Fig. 6*E*), suggesting that SESN2 may act as a transcriptional co-activator of Nrf2 target genes independently of Keap1.

As there is some concern in the literature whether the size of the mRNA predicted Nrf2 translation product (≈65 kDa) represents *bona fide* Nrf2 (34), we subsequently validated the anti-Nrf2 antibody employed in these experiments using immortalized MLFs from *Nrf2* knock out mice (23) and HeLa cells transduced with anti-Nrf2 shRNA. As shown Fig. 6*F*, the 65-kDa band detected by the R&D monoclonal antibody was missing in *Nrf2* KO MLFs, and its intensity was reduced in *NRF2* KD HeLa cells, confirming that this band represents monomeric Nrf2.

Nrf2 Inactivation Up-regulates Pdgfrβ—To test whether Nrf2 inactivation replicates the Pdgfrβ induction phenotype of *Sesn2* KO MLFs, we estimated ROS levels and Pdgfrβ expression in MLFs derived from *Nrf2* KO mice. As shown in Fig. 6*G*, *Nrf2* KO MLFs accumulated ROS and expressed significantly higher Pdgfrβ levels than the corresponding WT MLFs (Fig. 6, *H* and *I*), resulting in Pdgfrβ signal amplification in response to ligand stimulation (Fig. 6, *J* and *K*). This suggests that Sesn2, Nrf2, and the proteasome are all part of a redox-sensitive Pdgfrβ-suppressing pathway whose inactivation up-regulates Pdgfrβ. However, unlike previously reported Pdgfrβ activation by ROS-mediated inhibition of dedicated protein-tyrosine phosphatases (35, 36), the elevated phosphorylated Pdgfrβ (p-Pdgfrβ) levels in *Nrf2* KO MLFs were largely attributable to Pdgfrβ accumulation rather than enhanced phosphorylation. Thus, the Pdgfrβ/Gapdh ratio but not the p-Pdgfrβ/Pdgfrβ ratio was elevated in *Nrf2* KO MLFs (Fig. 6*K*).

Sesn2 Inactivation Up-regulates Nf-ya—We showed previously that the up-regulation of Pdgfrβ in the lungs of *Sesn2* KO mice occurred at both the mRNA and protein level (9). To test the possibility that mRNA induction is mediated by a Pdgfrβ transcription factor whose proteasomal degradation is delayed in Sesn2-depleted cells, we focused on the Nf-ya subunit of the Nf-y transcription factor complex, which controls basal Pdgfrβ gene transcription (37) and is degraded exclusively by the proteasome (38). Fig. 7, *A* and *B*, shows that Nf-ya and Pdgfrβ levels

were significantly increased in *Sesn2* KO MLFs. Most importantly, Nf-ya was also up-regulated in *Nrf2* KO MLFs (Fig. 7, *C* and *D*), suggesting that Nf-ya and Nrf2 operate within the same Sesn2/Pdgfrβ suppressor pathway (Fig. 7*E*).

Nrf2 Is Up-regulated in the Lungs of Individuals with COPD—Recently, we showed that SESN2 is up-regulated and PDGFRβ expression repressed in the lungs of individuals with advanced COPD (9), suggesting that the entire Sesn2/Pdgfrβ suppressor

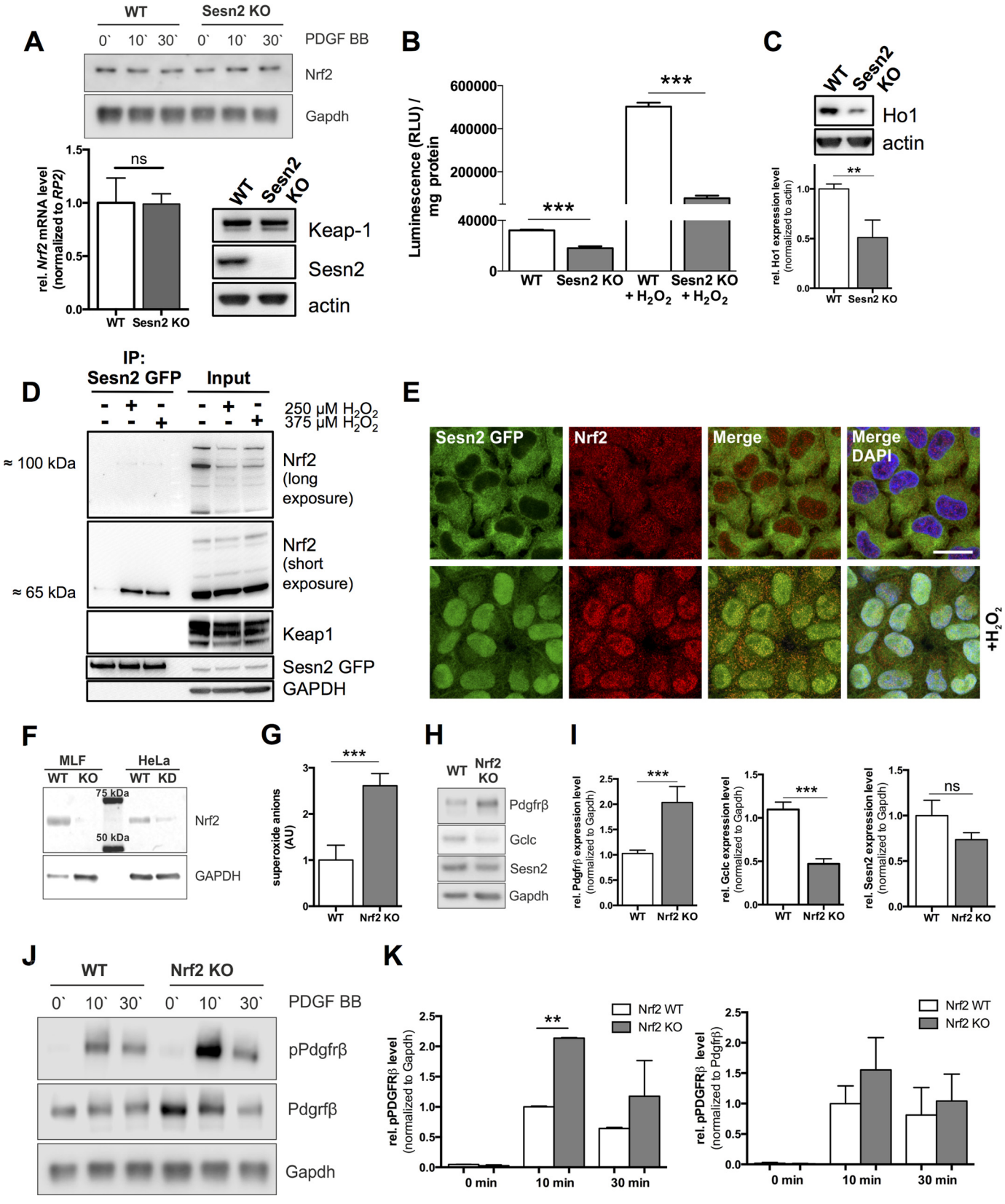

pathway (Fig. 7*E*) might be up-regulated in COPD lungs. Indeed, in contrast to previous reporting (39), we found NRF2 significantly up-regulated and KEAP1 repressed in COPD lungs when compared with healthy donor lungs (Fig. 8, *A* and *B*; see Table 1 for patient characteristics). Moreover, consistent with enhanced antioxidant defense, Nrf2 target genes such as GCLC, HO1, and PRX2 were also up-regulated in the COPD lungs, whereas the expression of the positive Nrf2 regulator DJ1 was not significantly different from normal lungs (Fig. 8, *A* and *B*). Finally, consistent with recent reporting (40) and in contrast to a previous study (53), proteasomal activity and subunit expression were not decreased in COPD lungs (Fig. 8, *C–F*).

DISCUSSION

We recently reported that Sesn2 interferes with the development of pulmonary emphysema by suppressing Pdgfrβ-regulated alveolar maintenance programs (9). Here, we identified the transcription factor Nrf2 and the 26 S proteasome as key components of a Sesn2/Pdgfrβ suppressor pathway and found that this pathway is highly up-regulated in lungs of individuals with advanced COPD.

In lung fibroblasts of mouse and human origin, inactivation of Sesn2 decreased proteasomal activity by inducing ROS formation via inhibition of Nrf2-controlled antioxidant gene expression. Decreased proteasomal degradation of Pdgfrβ and of its transcriptional activator Nf-ya resulted in Pdgfrβ accumulation and signal amplification in response to ligand stimulation (9).

In vitro and *in vivo* protein binding studies revealed that Sesn2 physically interacts with several 20 S proteasomal subunits including the catalytically active β1 and β5 subunits. Other oxidoreductases were also reported to associate with the 26 S proteasome. For example, thioredoxin-like 1 (Txn1) or thioredoxin-related protein of 32 kDa (TRP32) interacts with the 19 S regulatory subunit near the substrate binding site and was suggested to play a role in proteasome assembly (41–43). Likewise, the human flavin-dependent NADPH:quinone reductase (NQO1) interacts with the 20 S proteasome and protects transcription factors p53 and p73 from proteasomal degradation (31). Accordingly, Sesn2 could directly stimulate proteasomal activity by serving as a maturation factor that recruits proteasomal subunits for assembly. To our knowledge, the only other known interaction partner of the catalytically active proteasomal β subunits is proteassemblin (Ump1), which is involved in 20 S proteasome assembly (44, 45). In yeast, inactivation of the Ump1 homolog causes disordered proteasome assembly with abnormal subunit stoichiometry, incomplete propeptide processing, and reduced proteolytic activity (44). Similarly, the inactivation of Sesn2 might cause proteasome dysfunction by preventing its orderly assembly. Alternatively, Sesn2 interaction with 20 S proteasome might affect the structure of 20 S active sites and thus have an impact on proteasomal activity. Although this cannot be excluded by the present experiments, the recovery of proteasomal function in Sesn2-depleted cells by treatment with antioxidants such as NAC and Tempol suggests that Sesn2 also interferes indirectly with proteasomal function via ROS.

To scrutinize possible mechanisms of ROS accumulation in Sesn2-depleted cells, we used HeLa cells and mouse ESC-derived fibroblasts expressing EGFP-tagged Sesn2 from its endogenous chromosomal location, which enables generic tag-based proteomics under nearly physiological conditions. Although we found that Sesn2 physically interacts with peroxiredoxins, including over-oxidized peroxiredoxins, these interactions were effectively blocked by ROS. Thus, although the biological significance of the Sesn2/Prx interactions remains to be established, their inhibition by oxidative stress does not support the sulfinic acid reductase activity previously attributed to sestrins (3).

In agreement with a recent report (7), we found that Sesn2 regulates ROS metabolism by modulating the activity of Nrf2. Both *Sesn2* KO- and *Nrf2* KO MLFs accumulated ROS and up-regulated Pdgfrβ, confirming that Nrf2 is a downstream target of Sesn2. Indeed, experiments with nLAP-SESN2 expressing HeLa cells revealed that SESN2 co-localizes and physically interacts with NRF2, especially under oxidative stress conditions that simultaneously promoted a nuclear SESN2/NRF2 translocation. Because we could not detect a SESN2/KEAP1 interaction deemed essential for Nrf2 activation (7), this ROS-induced nuclear SESN2/NRF2 translocation suggests that Sesn2 may act as a transcriptional co-activator of Nrf2 target genes independently of Keap1.

Overall, we identified Nrf2, ROS, and the proteasome as central components of a novel signal transduction pathway employed by Sesn2 to suppress Pdgfrβ expression. Activation of NRF2 in the lungs of individuals with advanced COPD, which were shown to overexpress SESN2 (9), suggests that the Sesn2/Pdgfrβ suppressor pathway (Fig. 7*E*) is induced in COPD lungs and is responsible for repressing Pdgfrβ-controlled alveolar maintenance programs (9). In this context, it should be mentioned that activation of antioxidant defense mechanisms

FIGURE 6. **Nrf2 is a component of the Sesn2/Pdgfrβ suppressor pathway.** *A*, Nrf2 and Keap1 expression in WT and *Sesn2* KO MLFs. *Upper panel*, Nrf2 protein expression in response to PDGF-BB. *Lower left panel*, relative *Nrf2* mRNA levels in WT and *Sesn2* KO MLFs quantified by quantitative real-time PCR in three independent experiments. *ns*, not significant. *Lower right panel*, Keap1 protein expression in WT and *Sesn2* KO MLFs. *B*, suppression of Nrf2 activity in *Sesn2* KO MLFs. MLFs were transiently transfected with the pCignal Lenti-TRE-Reporter. After 48 h aliquots were treated with 125 μM H_2O_2 for 6 h, and luminescence was measured using a Mithras LB 940 plate reader. *RLU*, relative light units. *C*, Ho1 expression in WT and *Sesn2* KO MLFs. *Left panel*, Western blot. *Right panel*, densitometric quantification. *D*, nLAP-SESN2 IPs from HeLa cells probed with antibodies against Sesn2, Nrf2, and Keap1. Where indicated, cells were exposed for 6 h to H_2O_2 before the IPs. *E*, subcellular localization of Sesn2 and Nrf2 in nLAP-Sesn2 HeLa cells visualized by EGFP autofluorescence and indirect immunofluorescence staining before and after treatment with 125 μM H_2O_2. *Scale bar*: 20 μm. *F*, Western blot probed with monoclonal anti-Nrf2 antibody (R&D) showing absent and reduced Nrf2 expression in Nrf2-KO MLFs and Nrf2 knockdown HeLa cells, respectively. *G*, increased superoxide anion levels in *Nrf2* KO MLFs measured by EPR spectroscopy. Results are represented as the means ± S.E. of six independent measurements. *H*, representative Western blot showing expression levels of Pdgfrβ, Gclc, and Sesn2 in WT and *Nrf2* KO MLFs. *I*, densitometric quantification of Pdgfrβ (*left panel*) and Gclc (*middle panel*) and Sesn2 (*right panel*) expression in WT and *Nrf2* KO MLFs. *J*, representative Western blot showing phosphorylated Pdgfrβ (*pPdgfrβ*) in WT and *Nrf2* KO MLFs after treatment with 25 ng/ml recombinant human PDGF-BB. *K*, densitometric quantification of Pdgfrβ relative to GAPDH (*left panel*) and total Pdgfrβ (*right panel*). All results are represented as the means ± S.D. of three independent experiments. **, $p < 0.01$; ***, $p < 0.001$.

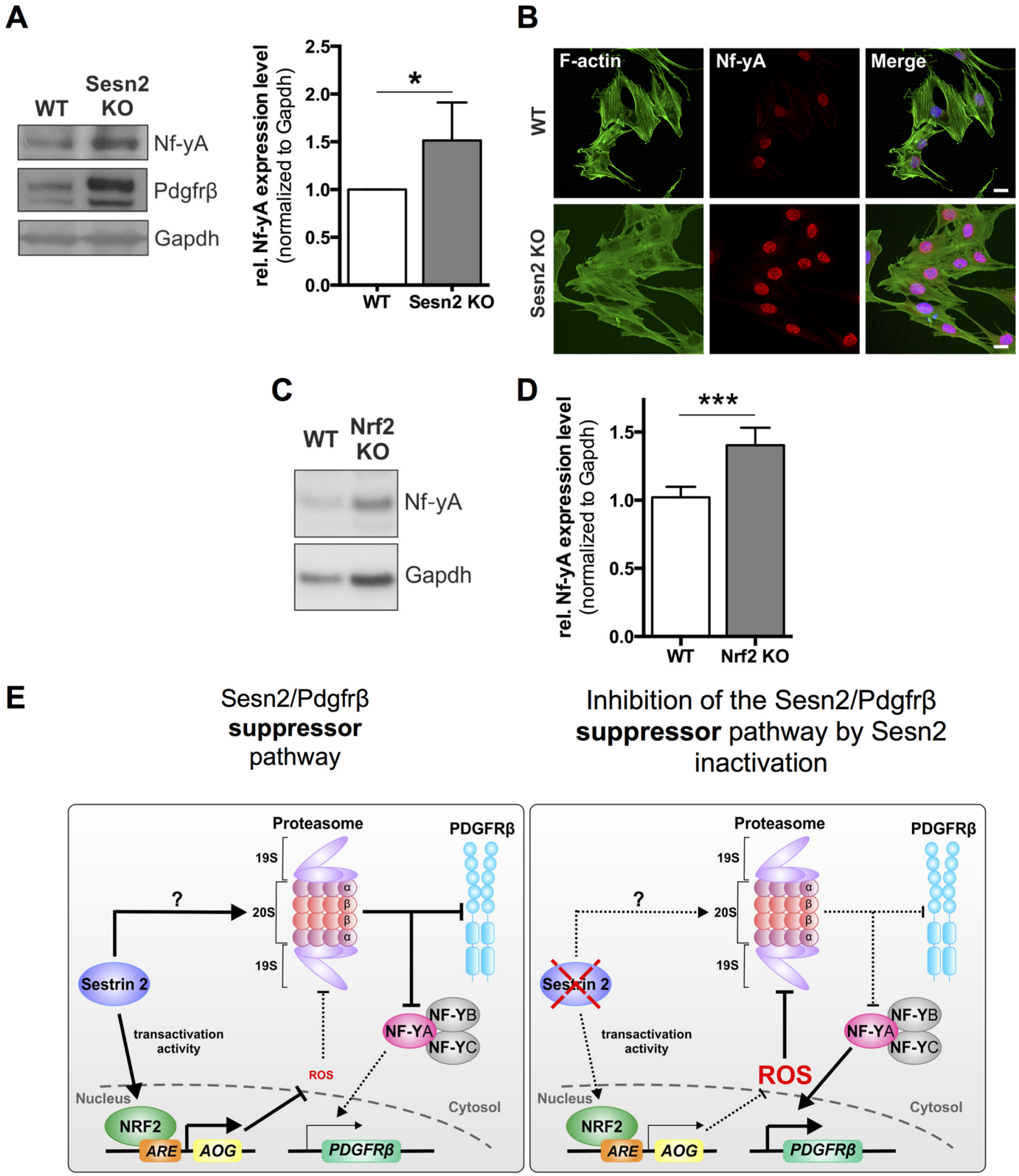

FIGURE 7. **Nf-ya is a component of the Sesn2/Pdgfrβ suppressor pathway.** *A*, expression of Nf-ya and Pdgfrβ in WT and *Sesn2* KO MLFs. *Left panel*, representative Western blot. *Right panel*, densitometric quantification. *B*, Nf-ya subcellular localization in WT and *Sesn2* KO MLFs visualized by immunofluorescence staining. Actin filaments were stained with fluorochrome-conjugated phalloidin. Note the nuclear accumulation of Nf-ya in *Sesn2* KO MLFs. *Scale bar*: 20 μm. *C* and *D*, expression of Nf-ya in WT and *Nrf2* KO MLFs. Shown is a representative Western blot (*C*) and densitometric quantification (*D*). All results are represented as the means ± S.D. of three independent experiments. $*p < 0.05$, $***p < 0.001$. *E*, schematic illustration of the Sesn2/Pdgfrβ suppressor pathway. *Left panel*, up-regulation of Sesn2 activates Nrf2 and the proteasome by direct binding and by suppressing ROS. The increased proteasomal degradation of Pdgfrβ and its transcriptional inducer Nf-ya reduces Pdgfrβ levels and Pdgfrβ signaling in response to ligand stimulation. *Right panel*, Sesn2 inactivation inhibits Nrf2 and proteasome functions resulting in Pdgfrβ accumulation and signal activation in response to ligand stimulation.

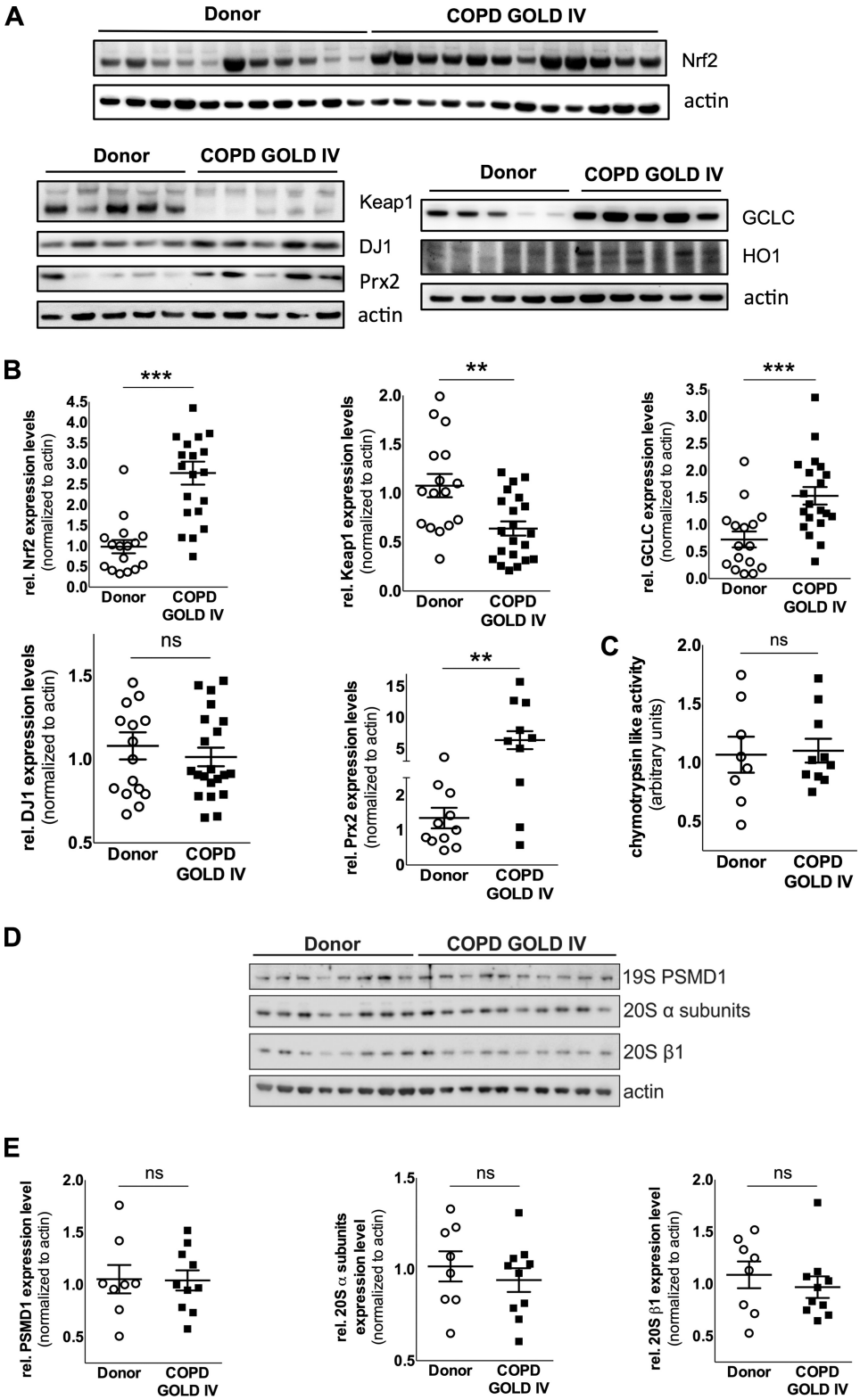

FIGURE 8. **Induction of the Sesn2/Pdgfrβ suppressor pathway in lungs of individuals with late stage COPD.** *A*, representative Western blots showing the expression of NRF2 (65 kDa), KEAP1, DJ1, PRX2, GCLC, and HO1 in lungs from healthy human donor and of individuals with late-stage COPD. *B*, densitometric quantification of protein levels: healthy donor ($n = 16$); COPD ($n = 20$). *ns*, not significant. *C*, CLA in lungs of healthy donors and individuals with advanced COPD: healthy donor ($n = 8$); COPD ($n = 10$). *D*, Western blot showing proteasomal subunit expression in lungs of healthy donors and individuals with advanced COPD. *E*, densitometric quantification of proteasomal subunit expression in lungs of donors and individuals with COPD: healthy donor ($n = 8$); COPD ($n = 10$). Each entry corresponds to one individual (for patient characteristics). Mean values ± S.E. are indicated by *straight lines*. **, $p < 0.01$; ***, $p < 0.001$.

TABLE 1

Clinical characteristics of normal donors and COPD patients

COPD IV, global initiative for chronic obstructive lung disease (GOLD) stage IV; FEV1, forced expiratory volume per second; FVC, forced vital capacity.

No.	Patient	Age	Sex	Pack/year	Diagnosis	FEV1/FVC	FEV1(l)	FEV1/predicted
						%		%
1	Donor	24	M					
2	Donor	52	F					
3	Donor	61	F					
4	Donor	26	M					
5	Donor	29	M					
6	Donor	55	F					
7	Donor	40	F					
8	Donor	42	M					
9	Donor	23	M					
10	Donor	63	F					
11	Donor	87	M					
12	Donor	34	F					
13	Donor	37	F					
14	Donor	31	M					
15	Donor	47	F					
16	Donor	64	M					
1	Smoker + COPD	53	M	39	COPD	49	1.56	14
2	Smoker + COPD	48	M	31	COPD	45	0.66	19
3	Smoker + COPD	58	M	70	COPD	31	0.86	20
4	Smoker + COPD	58	M	88	COPD	40	1.31	32
5	Smoker + COPD	59	M	5	COPD	63	0.76	22
6	Smoker + COPD	56	M	80	COPD	29	0.56	16
7	Smoker + COPD	55	M	35	COPD	38	0.55	13
8	Smoker + COPD	51	F	66	COPD	61	0.67	23
9	Smoker + COPD	63	M	37	COPD	40	0.93	20
10	Smoker + COPD	55	M	56	COPD	42	0.59	16
11	Smoker + COPD	50	F	60	COPD	41	0.57	23
12	Smoker + COPD	48	F	35	COPD	58	1.11	35
13	Smoker + COPD	45	M	60	COPD	34	1.00	20
14	Smoker + COPD	52	M	31	COPD	61	1.39	37
15	Smoker + COPD	57	M	38	COPD	35	0.42	12
16	Smoker + COPD	54	M	25	COPD	31	0.63	14
17	Smoker + COPD	52	M	20	COPD	54	0.56	13
18	Smoker + COPD	58	M	33	COPD	31	0.55	17
19	Smoker + COPD	60	M	34	COPD	46	0.82	24
20	Smoker + COPD	55	M	4	COPD	66	0.8	20

in COPD lungs is still a matter of debate. Although induction of antioxidant genes, including Nrf2, by chronic exposure to cigarette smoke was clearly documented in both airway epithelial cells and lung tissue (46–49), the picture is less clear in lungs of patients with COPD. Several genome-wide expression studies showed either up-regulation or no change in the expression of some (but not all) Nrf2-related antioxidant genes in COPD lungs (46, 50, 51), whereas other studies reported a decline in Nrf2 activity correlating with the severity of the disease (39). Our data showing that NRF2 is up-regulated in the lungs of individuals undergoing transplantation for late-stage COPD suggest that pharmacological NRF2 activators recently proposed for COPD treatment (52) should be used with caution.

Acknowledgments—We thank Lan Huang, University of California, Irvine, CA for providing the HTBH-hRpn11 HEK293 cells, Ivan Dikic, Institute of Biochemistry II, Goethe University Medical School, Frankfurt, Ritva Tikkanen, Institute of Biochemistry, Justus-Liebig University of Giessen, and Beate Böhm, Department of Rheumatology, Goethe University Medical School, Frankfurt for use of their equipment. We also thank Nadine Happel, Anna-Maria Scheder, and Elisa Pallasch for expert technical assistance.

REFERENCES

1. Budanov, A. V., Shoshani, T., Faerman, A., Zelin, E., Kamer, I., Kalinski, H., Gorodin, S., Fishman, A., Chajut, A., Einat, P., Skaliter, R., Gudkov, A. V., Chumakov, P. M., and Feinstein, E. (2002) Identification of a novel stress-responsive gene Hi95 involved in regulation of cell viability. *Oncogene* **21,** 6017–6031
2. Velasco-Miguel, S., Buckbinder, L., Jean, P., Gelbert, L., Talbott, R., Laidlaw, J., Seizinger, B., and Kley, N. (1999) PA26, a novel target of the p53 tumor suppressor and member of the GADD family of DNA damage and growth arrest inducible genes. *Oncogene* **18,** 127–137
3. Budanov, A. V., Sablina, A. A., Feinstein, E., Koonin, E. V., and Chumakov, P. M. (2004) Regeneration of peroxiredoxins by p53-regulated sestrins, homologs of bacterial AhpD. *Science* **304,** 596–600
4. Rhee, S. G., Chae, H. Z., and Kim, K. (2005) Peroxiredoxins: a historical overview and speculative preview of novel mechanisms and emerging concepts in cell signaling. *Free Radic. Biol. Med.* **38,** 1543–1552
5. Nyström, T., Yang, J., and Molin, M. (2012) Peroxiredoxins, gerontogenes linking aging to genome instability and cancer. *Genes Dev.* **26,** 2001–2008
6. Woo, H. A., Bae, S. H., Park, S., and Rhee, S. G. (2009) Sestrin 2 is not a reductase for cysteine sulfinic acid of peroxiredoxins. *Antioxid. Redox Signal.* **11,** 739–745
7. Bae, S. H., Sung, S. H., Oh, S. Y., Lim, J. M., Lee, S. K., Park, Y. N., Lee, H. E., Kang, D., and Rhee, S. G. (2013) Sestrins activate Nrf2 by promoting p62-dependent autophagic degradation of Keap1 and prevent oxidative liver damage. *Cell Metab.* **17,** 73–84
8. Kensler, T. W., Wakabayashi, N., and Biswal, S. (2007) Cell survival responses to environmental stresses via the Keap1-Nrf2-ARE pathway. *Annu. Rev. Pharmacol. Toxicol.* **47,** 89–116
9. Heidler, J., Fysikopoulos, A., Wempe, F., Seimetz, M., Bangsow, T., Tomasovic, A., Veit, F., Scheibe, S., Pichl, A., Weisel, F., Lloyd, K. C., Jaksch, P., Klepetko, W., Weissmann, N., and von Melchner, H. (2013) Sestrin-2, a repressor of PDGFRβ signalling, promotes cigarette-smoke-induced pulmonary emphysema in mice and is up-regulated in individuals with

COPD. *Dis. Model Mech.* **6,** 1378–1387
10. Liu, S. Y., Lee, Y. J., and Lee, T. C. (2011) Association of platelet-derived growth factor receptor β accumulation with increased oxidative stress and cellular injury in sestrin 2-silenced human glioblastoma cells. *FEBS Lett.* **585,** 1853–1858
11. Finley, D. (2009) Recognition and processing of ubiquitin-protein conjugates by the proteasome. *Annu. Rev. Biochem.* **78,** 477–513
12. Pickart, C. M., and Cohen, R. E. (2004) Proteasomes and their kin: proteases in the machine age. *Nat. Rev. Mol. Cell Biol.* **5,** 177–187
13. Deveraux, Q., Ustrell, V., Pickart, C., and Rechsteiner, M. (1994) A 26 S protease subunit that binds ubiquitin conjugates. *J. Biol. Chem.* **269,** 7059–7061
14. Husnjak, K., Elsasser, S., Zhang, N., Chen, X., Randles, L., Shi, Y., Hofmann, K., Walters, K. J., Finley, D., and Dikic, I. (2008) Proteasome subunit Rpn13 is a novel ubiquitin receptor. *Nature* **453,** 481–488
15. Lam, Y. A., Lawson, T. G., Velayutham, M., Zweier, J. L., and Pickart, C. M. (2002) A proteasomal ATPase subunit recognizes the polyubiquitin degradation signal. *Nature* **416,** 763–767
16. Schreiner, P., Chen, X., Husnjak, K., Randles, L., Zhang, N., Elsasser, S., Finley, D., Dikic, I., Walters, K. J., and Groll, M. (2008) Ubiquitin docking at the proteasome through a novel pleckstrin-homology domain interaction. *Nature* **453,** 548–552
17. Coux, O., Tanaka, K., and Goldberg, A. L. (1996) Structure and functions of the 20 S and 26 S proteasomes. *Annu. Rev. Biochem.* **65,** 801–847
18. Groll, M., Ditzel, L., Löwe, J., Stock, D., Bochtler, M., Bartunik, H. D., and Huber, R. (1997) Structure of 20 S proteasome from yeast at 2.4 A resolution. *Nature* **386,** 463–471
19. Wang, X., Yen, J., Kaiser, P., and Huang, L. (2010) Regulation of the 26 S proteasome complex during oxidative stress. *Sci. Signal.* **3,** ra88
20. Zalvide, J., Stubdal, H., and DeCaprio, J. A. (1998) The J domain of simian virus 40 large T antigen is required to functionally inactivate RB family proteins. *Mol. Cell. Biol.* **18,** 1408–1415
21. Schnütgen, F., Ehrmann, F., Poser, I., Hubner, N. C., Hansen, J., Floss, T., deVries, I., Wurst, W., Hyman, A., Mann, M., and von Melchner, H. (2011) Resources for proteomics in mouse embryonic stem cells. *Nat. Methods* **8,** 103–104
22. Hewitt, K. J., Shamis, Y., Carlson, M. W., Aberdam, E., Aberdam, D., and Garlick, J. A. (2009) Three-dimensional epithelial tissues generated from human embryonic stem cells. *Tissue Eng. Part A* **15,** 3417–3426
23. Itoh, K., Chiba, T., Takahashi, S., Ishii, T., Igarashi, K., Katoh, Y., Oyake, T., Hayashi, N., Satoh, K., Hatayama, I., Yamamoto, M., and Nabeshima, Y. (1997) An Nrf2/small Maf heterodimer mediates the induction of phase II detoxifying enzyme genes through antioxidant response elements. *Biochem. Biophys. Res. Commun.* **236,** 313–322
24. Wempe, F., De-Zolt, S., Koli, K., Bangsow, T., Parajuli, N., Dumitrascu, R., Sterner-Kock, A., Weissmann, N., Keski-Oja, J., and von Melchner, H. (2010) Inactivation of sestrin 2 induces TGF-β signaling and partially rescues pulmonary emphysema in a mouse model of COPD. *Dis. Model Mech.* **3,** 246–253
25. Tomasovic, A., Traub, S., and Tikkanen, R. (2012) Molecular networks in FGF signaling: flotillin-1 and cbl-associated protein compete for the binding to fibroblast growth factor receptor substrate 2. *PLoS ONE* **7,** e29739
26. Mittal, M., Roth, M., König, P., Hofmann, S., Dony, E., Goyal, P., Selbitz, A. C., Schermuly, R. T., Ghofrani, H. A., Kwapiszewska, G., Kummer, W., Klepetko, W., Hoda, M. A., Fink, L., Hänze, J., Seeger, W., Grimminger, F., Schmidt, H. H., and Weissmann, N. (2007) Hypoxia-dependent regulation of nonphagocytic NADPH oxidase subunit NOX4 in the pulmonary vasculature. *Circ. Res.* **101,** 258–267
27. Kurrle, N., Völlner, F., Eming, R., Hertl, M., Banning, A., and Tikkanen, R. (2013) Flotillins directly interact with gamma-catenin and regulate epithelial cell-cell adhesion. *PLoS ONE* **8,** e84393
28. Mori, S., Kanaki, H., Tanaka, K., Morisaki, N., and Saito, Y. (1995) Ligand-activated platelet-derived growth factor β-receptor is degraded through proteasome-dependent proteolytic pathway. *Biochem. Biophys. Res. Commun.* **217,** 224–229
29. Chen, Y., Dai, X., Haas, A. L., Wen, R., and Wang, D. (2006) Proteasome-dependent down-regulation of activated Stat5A in the nucleus. *Blood* **108,** 566–574
30. Gregory, M. A., and Hann, S. R. (2000) c-Myc proteolysis by the ubiquitin-proteasome pathway: stabilization of c-Myc in Burkitt's lymphoma cells. *Mol. Cell. Biol.* **20,** 2423–2435
31. Asher, G., and Shaul, Y. (2005) p53 proteasomal degradation: poly-ubiquitination is not the whole story. *Cell Cycle* **4,** 1015–1018
32. Wang, X., Chen, C. F., Baker, P. R., Chen, P. L., Kaiser, P., and Huang, L. (2007) Mass spectrometric characterization of the affinity-purified human 26 S proteasome complex. *Biochemistry* **46,** 3553–3565
33. Poser, I., Sarov, M., Hutchins, J. R., Hériché, J. K., Toyoda, Y., Pozniakovsky, A., Weigl, D., Nitzsche, A., Hegemann, B., Bird, A. W., Pelletier, L., Kittler, R., Hua, S., Naumann, R., Augsburg, M., Sykora, M. M., Hofemeister, H., Zhang, Y., Nasmyth, K., White, K. P., Dietzel, S., Mechtler, K., Durbin, R., Stewart, A. F., Peters, J. M., Buchholz, F., and Hyman, A. A. (2008) BAC TransgeneOmics: a high-throughput method for exploration of protein function in mammals. *Nat. Methods* **5,** 409–415
34. Lau, A., Tian, W., Whitman, S. A., and Zhang, D. D. (2013) The predicted molecular weight of Nrf2: it is what it is not. *Antioxid. Redox Signal.* **18,** 91–93
35. Choi, M. H., Lee, I. K., Kim, G. W., Kim, B. U., Han, Y. H., Yu, D. Y., Park, H. S., Kim, K. Y., Lee, J. S., Choi, C., Bae, Y. S., Lee, B. I., Rhee, S. G., and Kang, S. W. (2005) Regulation of PDGF signalling and vascular remodelling by peroxiredoxin II. *Nature* **435,** 347–353
36. Dagnell, M., Frijhoff, J., Pader, I., Augsten, M., Boivin, B., Xu, J., Mandal, P. K., Tonks, N. K., Hellberg, C., Conrad, M., Arnér, E. S., and Östman, A. (2013) Selective activation of oxidized PTP1B by the thioredoxin system modulates PDGF-β receptor tyrosine kinase signaling. *Proc. Natl. Acad. Sci. U.S.A.* **110,** 13398–13403
37. Ishisaki, A., Murayama, T., Ballagi, A. E., and Funa, K. (1997) Nuclear factor Y controls the basal transcription activity of the mouse platelet-derived growth factor β receptor gene. *Eur. J. Biochem.* **246,** 142–146
38. Manni, I., Caretti, G., Artuso, S., Gurtner, A., Emiliozzi, V., Sacchi, A., Mantovani, R., and Piaggio, G. (2008) Posttranslational regulation of NF-YA modulates NF-Y transcriptional activity. *Mol. Biol. Cell* **19,** 5203–5213
39. Malhotra, D., Thimmulappa, R., Navas-Acien, A., Sandford, A., Elliott, M., Singh, A., Chen, L., Zhuang, X., Hogg, J., Pare, P., Tuder, R. M., and Biswal, S. (2008) Decline in NRF2-regulated antioxidants in chronic obstructive pulmonary disease lungs due to loss of its positive regulator, DJ-1. *Am. J. Respir Crit. Care Med.* **178,** 592–604
40. Baker, T. A., Bach, H. H., 4th, Gamelli, R. L., Love, R. B., and Majetschak, M. (2014) Proteasomes in lungs from organ donors and patients with end-stage pulmonary diseases. *Physiol. Res.* **63,** 311–319
41. Andersen, K. M., Madsen, L., Prag, S., Johnsen, A. H., Semple, C. A., Hendil, K. B., and Hartmann-Petersen, R. (2009) Thioredoxin Txnl1/TRP32 is a redox-active cofactor of the 26 S proteasome. *J. Biol. Chem.* **284,** 15246–15254
42. Wiseman, R. L., Chin, K. T., Haynes, C. M., Stanhill, A., Xu, C. F., Roguev, A., Krogan, N. J., Neubert, T. A., and Ron, D. (2009) Thioredoxin-related protein 32 is an arsenite-regulated thiol reductase of the proteasome 19 S particle. *J. Biol. Chem.* **284,** 15233–15245
43. Hendil, K. B., Kriegenburg, F., Tanaka, K., Murata, S., Lauridsen, A. M., Johnsen, A. H., and Hartmann-Petersen, R. (2009) The 20 S proteasome as an assembly platform for the 19 S regulatory complex. *J. Mol. Biol.* **394,** 320–328
44. Ramos, P. C., Höckendorff, J., Johnson, E. S., Varshavsky, A., and Dohmen, R. J. (1998) Ump1p is required for proper maturation of the 20 S proteasome and becomes its substrate upon completion of the assembly. *Cell* **92,** 489–499
45. Jayarapu, K., and Griffin, T. A. (2004) Protein-protein interactions among human 20 S proteasome subunits and proteassemblin. *Biochem. Biophys. Res. Commun.* **314,** 523–528
46. Pierrou, S., Broberg, P., O'Donnell, R. A., Pawłowski, K., Virtala, R., Lindqvist, E., Richter, A., Wilson, S. J., Angco, G., Möller, S., Bergstrand, H., Koopmann, W., Wieslander, E., Strömstedt, P. E., Holgate, S. T., Davies, D. E., Lund, J., and Djukanovic, R. (2007) Expression of genes involved in oxidative stress responses in airway epithelial cells of smokers with chronic obstructive pulmonary disease. *Am. J. Respir. Crit. Care Med.* **175,** 577–586
47. Hübner, R. H., Schwartz, J. D., De Bishnu, P., Ferris, B., Omberg, L., Mezey,

J. G., Hackett, N. R., and Crystal, R. G. (2009) Coordinate control of expression of Nrf2-modulated genes in the human small airway epithelium is highly responsive to cigarette smoking. *Mol. Med.* **15,** 203–219
48. Müller, T., and Hengstermann, A. (2012) Nrf2: friend and foe in preventing cigarette smoking-dependent lung disease. *Chem. Res. Toxicol.* **25,** 1805–1824
49. Zhu, L., Barrett, E. C., Barret, E. C., Xu, Y., Liu, Z., Manoharan, A., and Chen, Y. (2013) Regulation of Cigarette Smoke (CS)-Induced Autophagy by Nrf2. *PLoS ONE* **8,** e55695
50. Comandini, A., Marzano, V., Curradi, G., Federici, G., Urbani, A., and Saltini, C. (2010) Markers of anti-oxidant response in tobacco smoke exposed subjects: a data-mining review. *Pulm. Pharmacol. Ther.* **23,** 482–492
51. Brandsma, C. A., van den Berge, M., Postma, D. S., Jonker, M. R., Brouwer, S., Paré, P. D., Sin, D. D., Bossé, Y., Laviolette, M., Karjalainen, J., Fehrmann, R. S., Nickle, D. C., Hao, K., Spanjer, A. I., Timens, W., and Franke, L. (2015) A large lung gene expression study identifying fibulin-5 as a novel player in tissue repair in COPD. *Thorax* **70,** 21–32
52. Biswal, S., Thimmulappa, R. K., and Harvey, C. J. (2012) Experimental therapeutics of Nrf2 as a target for prevention of bacterial exacerbations in COPD. *Proc. Am. Thorac. Soc.* **9,** 47–51
53. Malhotra, D., Thimmulappa, R., Vij, N., Navas-Acien, A., Sussan, T., Merali, S., Zhang, L., Kelsen, S. G., Myers, A., Wise, R., Tuder, R., and Biswal, S. (2009) Expression of concern: Heightened endoplasmic reticulum stress in the lungs of patients with chronic obstructive pulmonary disease: the role of Nrf2-regulated proteasomal activity. *Am. J. Respir. Crit. Care Med.* **180,** 1196–1207